A MODEL FOR QUASI-PERIODIC SIGNALS WITH APPLICATION TO RAIN ESTIMATION FROM MICROWAVE LINK GAIN

Christoph Reller[1], *Hans-Andrea Loeliger*[1], *Juan Pablo Marín Díaz*[2]

[1] Dept. ITET, ETH Zurich, 8092 Zürich, Switzerland, Email: {reller, loeliger}@isi.ee.ethz.ch
[2] Latinno Institute for Data Processing and Analysis, Bogota , Colombia, Email: j.marin@javeriana.edu.co

ABSTRACT

It has been observed that rainfall may be estimated from the attenuation of microwave links. In this paper, we propose a new approach to this problem (for a single microwave link), which is based on a dynamical model of the attenuation without rain. This dry-air model combines local smoothing with quasi-periodicity over 24 hours. Rainfall causes large deviations of the attenuation from this dry-air model, and the rainfall can be estimated from these deviations.

The proposed approach yields practical algorithms that are shown to work well on real data. We propose both an iterative offline algorithm for estimating past rainfall and an online algorithm for estimating present rainfall. Both algorithms can cope with irregular sampling and intervals of missing data.

The factor graph approach of this paper demonstrates a number of modeling techniques that are not quite standard—including extensive use of "soft" equality constraints and forgetting factors—and may therefore be of interest beyond the immediate application.

1. INTRODUCTION

This paper has a dual purpose: on the one hand, it proposes a new solution to a practical problem; on the other hand, it demonstrates the versatility of some factor graph modeling techniques that are not quite standard.

We begin with the former. It is well known that outdoor microwave links commonly used in commercial telecommunication networks suffer from attenuation due to rain [1]. From this observation, it has been suggested to estimate rainfall rates based on available attenuation data of microwave links [2]. Indeed, estimating rainfall rates in this way would be a welcome complement to rain gauges and rain radar measurements [2, 3].

However, estimating rainfall from attenuation data has remained a challenge. The nature of the problem is illustrated by the gray line in Figure 6, which shows the attenuation (or rather the gain) of a microwave link over 5 days. The deep jags in the figure are due to heavy rain; without rain, the attenuation fluctuates (more or less) smoothly within some fixed range. The dry-air baseline exhibits some degree of periodicity with a period of 24 hours, which is due to the daily cycle of temperature, humidity, and air pressure.

Commonly, estimating the rainfall rate from such attenuation data involves three separate tasks [2,4,5]. The first task is to classify the data into segments with rain and segments without rain. The second task is to estimate the smoothed baseline within each rainy segment, which is subtracted from the measured attenuation; the result is a net attenuation due to rain only. The third task is to estimate the rainfall rate based on this net attenuation.

In this paper, we will focus on the first two tasks, which will be addressed jointly. The third task has been the focus of prior work both in the context of rainfall rate estimation [2,3,6] and for modelling rain attenuation [1,7], and will not be addressed in this paper.

In contrast to all prior work, we will explicitly model and use the daily cycle. While elaborate stochastic models for rain attenuation exist [7], none of the published rain estimation algorithms [2–6] explicitly uses the daily cycle.

From the proposed model, we derive practical algorithms to estimate the dry-air baseline. We propose both an iterative offline algorithm for estimating past rainfall and an online algorithm for estimating present rainfall. Both algorithms can cope with irregular sampling and intervals of missing data, and both algorithms are shown to work well on real data.

Our model for the dry-air baseline combines local smoothness constraints with periodicity constraints. The former consist of a line model whose parameters are allowed to slowly vary over time; the latter penalizes deviations from periodicity of the parameters of the line model. Both parts use soft-equality constraints that are implemented by means of forgetting factors (cf. [8]). In consequence, the overall model is not, strictly speaking, a statistical model, but a collection of smoothly connected "local" statistical models, one for each time instant.

An alternative factor graph model for quasi-periodic signals was proposed in [9].

The paper is structured as follows. The proposed factor graph model for the dry-air baseline model is presented in Section 2. The resulting iterative algorithms are described in Section 3. Some empirical results are reported in Section 4, and Section 5 concludes the paper. The paper assumes some familiarity with factor graphs [10].

2. THE MODEL

We will express the proposed model for the dry-air baseline in terms of factor graphs as in [10]. The model consists of two sub-models: one sub-model for local smoothness and one sub-model for (quasi-) periodicity. The resulting factor graph is shown in Figure 1, which will be explained in the following. Note that the overall model is not generative.

We will use the set of discrete time instants $\{t_m\}_{m\in\{1,\dots,M\}}$, which is partitioned into two subsets $\{t_k\}_{k\in\mathcal{K}}$ and $\{t_\ell\}_{\ell\in\mathcal{L}}$, where $\mathcal{K}$ and $\mathcal{L}$ are index sets, as illustrated in Figure 1. The subset $\{t_k\}_{k\in\mathcal{K}}$ contains the time stamps of the given attenuation data $\{y_k\}_{k\in\mathcal{K}}$. The subset $\{t_\ell\}_{\ell\in\mathcal{L}}$ describes a regular grid containing N time instants per period T, where $T = 1$ day.

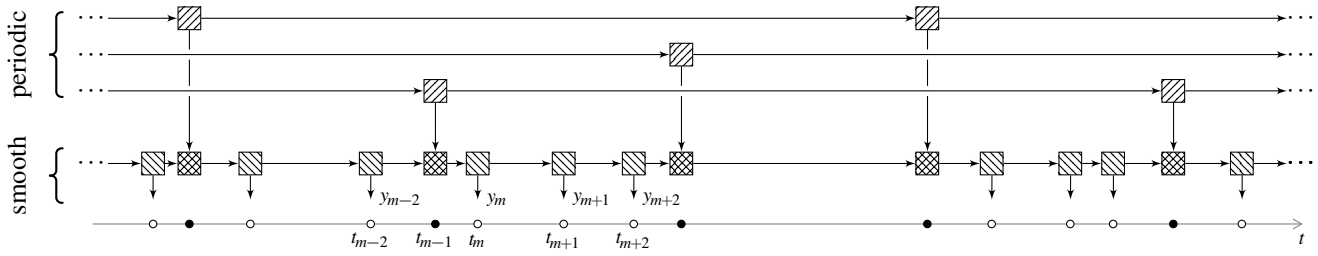

Figure 1: Example overall factor graph with sets of time instants $\{t_k\}_{k\in\mathcal{K}}$ and $\{t_\ell\}_{\ell\in\mathcal{L}}$ depicted as "$\circ$" and "$\bullet$" respectively. The boxes ▨, ▩, and ▨ are defined in Figures 3–2.

To model smoothness, we will use a local line model in state space form. A noisy version $S_\ell \in \mathbb{R}^2$ of the state of this line model is used by the "periodic" sub-model to impose the soft-equality constraints

$$S_\ell \overset{\beta}{=} S_{\ell'}\,, \quad \forall\,(\ell,\ell') \in \mathcal{L}^2 : t_\ell - t_{\ell'} = T\,, \tag{1}$$

where the soft equality $\overset{\beta}{=}$ indicates the application of a forgetting factor β. Figure 2 shows the factor graph representation of (1).

As in [8], we define the action of a forgetting factor in terms of manipulation of sum-product messages in the factor graph. Specifically, on every edge marked with square brackets "$][$" in Figures 2–4, the forward as well as the backward message is taken to the power of the forgetting factor. We restrict forgetting factors to be smaller than 1 but close to 1. The application of forgetting factors thus relaxes strict global properties, such as periodicity, into local properties.

The "smooth" sub-model consists of the following second-order linear state space model:

$$X_m \overset{\gamma_m}{=} A_m X_{m-1}\,, \quad \forall\, m \in \{2,\ldots,M\}\,, \tag{2}$$

where

$$A_m \triangleq \begin{pmatrix} 1 & t_m - t_{m-1} \\ 0 & 1 \end{pmatrix} \tag{3}$$

is the time-varying state transition matrix. With this choice of A_m, the state $X_m \in \mathbb{R}^2$ in (2) models a straight line as a function of time, i.e. $[X_m]_1$ contains the line value at time t_m and $[X_m]_2$ contains the line slope.

The soft equality $\overset{\gamma_m}{=}$ in (2) again indicates the use a forgetting factor $\gamma_m \triangleq \rho^{t_m - t_{m-1}}$, where the parameter ρ is the forgetting factor per unit time. As before, the application of a forgetting factor relaxes the strict line model into a local model. We model the observed data at time instants $\{t_k\}_{k\in\mathcal{K}}$ as noisy observations of the state:

$$Y_k = CX_k + Z_k\,, \quad \forall\, k \in \mathcal{K}\,, \tag{4}$$

where $C \triangleq (1,0)$ and Z_k is zero-mean additive white Gaussian noise. We will explain in Section 3 how the variance of this noise is chosen. Figure 3 depicts the factor graph representation of (2) and (4).

To complete our model, we noisily connect the states of the "periodic" sub-model and the "smooth" sub-model at time instants $\{t_\ell\}_{\ell\in\mathcal{L}}$ as

$$S_\ell = X_\ell + U_\ell\,, \quad \forall\, \ell \in \mathcal{L}\,, \tag{5}$$

where U_ℓ is zero-mean white Gaussian noise with diagonal covariance matrix $V_U \triangleq \mathrm{diag}(\sigma^2_{U,0}, \sigma^2_{U,1})$. The factor graph representation of (2) and (5) is shown in Figure 4.

We now have defined the overall factor graph in Figure 1 with Figures 2–4 inserted into the respective boxes. Note that the exact topology of the overall factor graph depends on the time stamps $\{t_k\}_{k\in\mathcal{K}}$ and the number of connections N per period T.

We conclude this section with two remarks. Firstly, note that the effect of a forgetting factor is similar (but, in this case, not equal) to additive state noise.

Secondly, it is not difficult to extend the line model (2) and (4) to higher order polynomials, but it does not seem to be helpful in this application.

3. ALGORITHMS

Given the observations $\{y_k\}_{k\in\mathcal{K}}$ of the microwave link attenuation with corresponding time stamps t_k, we wish to compute estimates $\hat{y}_k$ of the dry-air baseline and class labels $c_k \in \{0,1\}$ where 0 means "rainy" and 1 means "dry".

We propose both an iterative offline algorithm for estimating past rainfall and an online algorithm for estimating present rainfall. For the offline algorithm, the whole data y_k for $k \in \mathcal{K}$ is processed at once.

For the online algorithm, data arrives sequentially in a stream, and the output is produced in a stream too. Instead of using a block-based version of the offline algorithm, we propose a non-iterative algorithm where definitive estimates $\hat{y}_k$ and class labels c_k are calculated once the data item y_k has arrived.

Both algorithms can cope with irregular sampling and intervals of missing data, and both algorithms are shown to work well on real data.

We have not yet explained how the distinction between "dry" and "rainy" data items is modelled. We propose to achieve this by considering a time-varying variance $\sigma^2_{c_k}$ of the observation noise Z_k in (4), depending on the class label c_k. Since we expect "rainy" data to have a larger offset from the dry-air baseline than "dry" data we choose $\sigma^2_0 \gg \sigma^2_1$. All model and algorithm parameters are listed in Table 1.

3.1 Message Passing and Classification

The algorithms presented here are constructed from sum-product message passing in the overall factor graph of Figure 1 with Figures 2–4 inserted into the respective boxes. Every edge in the graph corresponds to a variable and is associated with a forward message sent in the same direction as

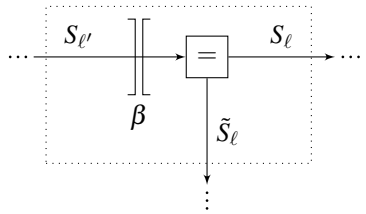

Figure 2: Definition of the boxes in Figures 1 and 5.

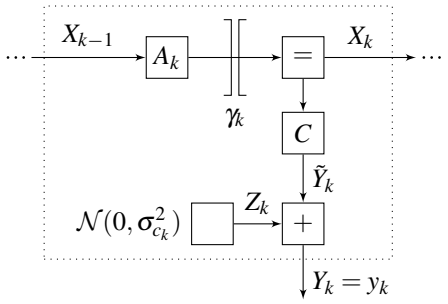

Figure 3: Definition of the boxes in Figures 1 and 5.

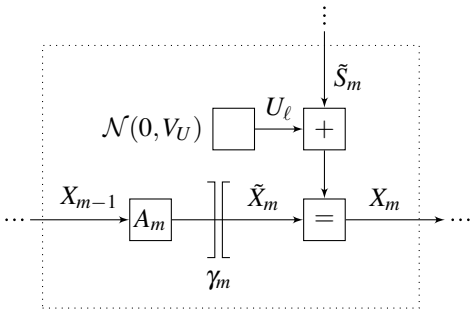

Figure 4: Definition of the boxes in Figures 1 and 5.

the direction of the edge and a backward message sent in the opposite direction. We use arrows to distinguish between forward messages ($\vec{\cdot}$) and backward messages ($\overleftarrow{\cdot}$). Messages leaving a node on some edge are calculated from messages entering the node on all other edges using the sum-product rule. (See [10] for the use of the sum-product rule and Gaussian factor graphs.)

In this graph all messages are scaled and potentially degenerate (multivariate) Gaussian probability density functions. E.g., the forward message on some edge X is

$$\vec{\mu}_X(x) \propto e^{-(x-\vec{m}_X)^{\mathrm{T}}\vec{W}_X(x-\vec{m}_X)/2}, \tag{6}$$

where $\vec{m}_X$ is the mean vector, $\vec{W}_X^{-1}$ is the covariance matrix (if it exists), and $\propto$ denotes equality up to a constant. Any message is thus parameterized by its mean and its inverse covariance matrix. If X is a scalar then we write $\vec{\sigma}_X^2$ instead of $\vec{W}_X^{-1}$.

For messages of the form (6), the application of a forgetting factor γ amounts to multiplying $\vec{W}_X$ by γ. On every edge with square brackets "]" in Figures 2–4, the forward as well as the backward message undergoes this manipulation. For all nodes in Figures 2–4, the message update rules for Gaussian messages are listed and derived in [10]. An estimate $\hat{x}$ of some variable X in the graph is calculated as $\hat{x} = \operatorname{argmax}_x \vec{\mu}_X(x)\overleftarrow{\mu}_X(x)$.

We propose to alternate between

1. calculating $\vec{\mu}_{\tilde{Y}_k}$, $\overleftarrow{\mu}_{\tilde{Y}_k}$, and

$$\hat{y}_k = \operatorname*{argmax}_y \vec{\mu}_{\tilde{Y}_k}(y)\overleftarrow{\mu}_{\tilde{Y}_k}(y), \quad \forall\, k \in \mathcal{K}, \tag{7}$$

   for fixed class labels c_k and
2. updating class labels c_k based on the messages $\vec{\mu}_{\tilde{Y}_k}$.

For fixed class labels c_k the messages $\vec{\mu}_{\tilde{Y}_k}$ and $\overleftarrow{\mu}_{\tilde{Y}_k}$ in (7) are calculated by message passing in the overall graph. As a by-product of Step 1, we calculate state estimates $\hat{x}_m = \operatorname{argmax}_x \vec{\mu}_{X_m}(x)\overleftarrow{\mu}_{X_m}(x)$ for $m = 1,\ldots,M$, and hence we are able to extract dry-air baseline estimates $[\hat{x}_\ell]_1$ at time instants t_ℓ for $\ell \in \mathcal{L}$ where no data y_k is present.

For $k \in \mathcal{K}$, the message $\vec{\mu}_{Y_k}(y)$ represents a probability density function on Y_k given the observations $Y_j = y_j$ for all $j \in \mathcal{K} \setminus \{k\}$ and the overall model. We classify the data item y_k as "rainy" if the value y_k lies outside of a confidence interval $[\vec{m}_{Y_k} - \theta\vec{\sigma}_{Y_k}, \infty)$, i.e:

$$c_k = \begin{cases} 0 & \text{if} \quad y_k < \eta_k \\ 1 & \text{else} \end{cases}, \quad \eta_k \triangleq \vec{m}_{Y_k} - \theta\vec{\sigma}_{Y_k}, \tag{8}$$

where θ is a parameter of the algorithm. Note that in this application we only choose "rainy" if y_k is less than the detection threshold η_k. If the outliers were expected to lie below as well as above the dry-air baseline then we would consider a confidence interval $[\vec{m}_{Y_k} - \theta\vec{\sigma}_{Y_k}, \vec{m}_{Y_k} + \theta\vec{\sigma}_{Y_k}]$. Also note that the threshold η_k is time-varying and adapts automatically to non-uniform time stamps and hence to missing data.

3.2 Offline Algorithm

Let R_1, R_2 be the number of recursions in the loops. The algorithm is the following:

1. **`init`**
2. Do R_1 times (or until convergence): **`smooth`**
3. Do R_2 times:
   (a) **`periodic`**
   (b) Do R_1 times (or until convergence): **`smooth`**
4. **`end`**

The subroutines (with reference to Figures 1–4) are:

`init`: Set $c_k = 1$ for all $k \in \mathcal{K}$. Set $\vec{W}_{\tilde{S}_\ell} = 0$ for all $\ell \in \mathcal{L}$. Set $\vec{W}_{X_0} = 0$ and $\overleftarrow{W}_{X_M} = 0$.

`smooth`: Given c_k for all $k \in \mathcal{K}$ and $\vec{\mu}_{\tilde{S}_\ell}$ for all $\ell \in \mathcal{L}$, do forward and backward message passing in the "smooth" sub-model. Calculate $\vec{\mu}_{Y_k}$ for all $k \in \mathcal{K}$, and $\overleftarrow{\mu}_{\tilde{S}_\ell}$ for all $\ell \in \mathcal{L}$. For all $k \in \mathcal{K}$ apply the classification rule (8) to update c_k. If c_k is unchanged for all $k \in \mathcal{K}$ then declare convergence.

`periodic`: Given $\overleftarrow{\mu}_{\tilde{S}_\ell}$ for all $\ell \in \mathcal{L}$, do forward and backward message passing in all N state spaces of the "periodic" sub-model. Calculate $\vec{\mu}_{\tilde{S}_\ell}$ for all $\ell \in \mathcal{L}$.

`end`: Calculate $\hat{y}_k$ for all $k \in \mathcal{K}$ and $[\hat{x}_\ell]_1$ for all $\ell \in \mathcal{L}$.

3.3 Online Algorithm

We assume that the data item y_k with time stamp t_k has arrived and we want to compute an estimate $\hat{y}_k$ and a class label c_k. The corresponding factor graph is depicted in Figure 5. In contrast to the offline model in Figure 1, the factor graph now

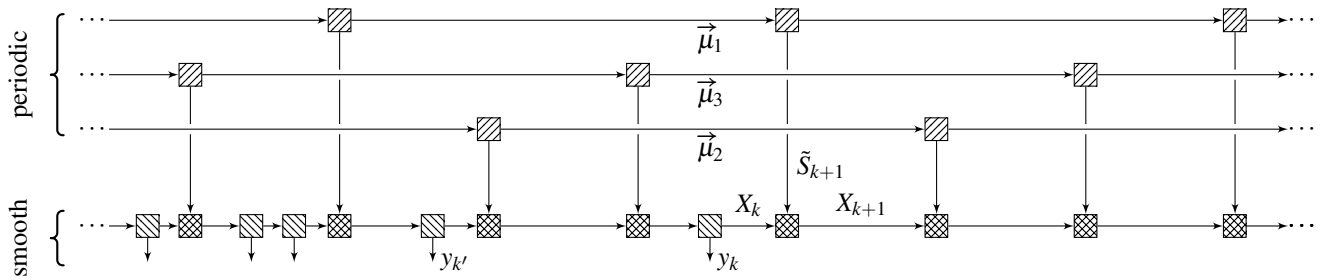

Figure 5: Example overall factor graph for the online algorithm. The boxes ▨, ▩, and ▨ are defined in Figures 3–2.

extends infinitely from t_k on towards the future. The purpose of this is, that we want to consider the backward message $\overleftarrow{\mu}_{X_k}$ without having future observations, i.e., only due to the "periodic" sub-model.

The factor graph in Figure 5 still has cycles and therefore algorithms based directly on this graph are still iterative. Moreover, since the graph extends infinitely into the future a direct application of message passing is not practical. To make the algorithm non-iterative and practical we make the following simplifications:

1. No iterations are done for classification.
2. For all $\ell \in \mathcal{L}$, the message $\overleftarrow{\mu}_{\tilde{S}_\ell}$ is calculated assuming a neutral message $\overleftarrow{\mu}_{X_\ell}$, i.e., $\overleftarrow{\mu}_{X_\ell}(x) = 1$. In contrast, for all $k \in \mathcal{K}$, the message $\vec{\mu}_{Y_k}$, and hence the classification and the dry-air baseline estimation, is calculated from a non-neutral message $\overleftarrow{\mu}_{X_k}$. We formulate the calculation of this message below.
3. The messages $\overleftarrow{\mu}_{S_\ell}$ are assumed to be neutral, i.e., $\overleftarrow{\mu}_{S_\ell}(s) = 1$ for all $\ell \in \mathcal{L}$. Hence, the message $\vec{\mu}_{\tilde{S}_\ell}$ is always calculated as $\vec{\mu}_{\tilde{S}_\ell}(s) = \vec{\mu}_{S_{\ell'}}(s)^\beta$, where ℓ' is chosen such that $t_{\ell'} = t_\ell - T$.
4. For all $\ell > k$ we select the connection noise variance in the node $\mathcal{N}(0, V_U)$ as $V_U = 0$ (see Figure 4).

Simplifications 3 and 4 allow us to formulate the (non-neutral) message $\overleftarrow{\mu}_{X_k}$ despite the infinite extension of the graph towards the future. In the following we formulate the message $\overleftarrow{\mu}_{\tilde{X}_{k+1}}$ (see Figure 4) from which $\overleftarrow{\mu}_{X_k}$ can easily be obtained.

We start by defining $\vec{\mu}_n \triangleq \vec{\mu}_{S_{\ell_n}}$ (as depicted in Figure 5), where ℓ_n is chosen such that $t_{k+1} - t_{\ell_n} = (N-n+1)T/N$ for $n = 1, \ldots, N$. Let $\vec{W}_n$ and $\vec{m}_n$ be the inverse covariance matrix and the mean vector of $\vec{\mu}_n$ respectively.

It can be shown, that $\overleftarrow{W}_{\tilde{X}_{k+1}}$ is given by the solution of the Lyapunov equation

$$\overleftarrow{W}_{\tilde{X}_{k+1}} - \beta\rho^T \left(A^N\right)^{\mathrm{T}} \overleftarrow{W}_{\tilde{X}_{k+1}} A^N = \sum_{n=1}^{N} \rho^{nT/N} (A^n)^{\mathrm{T}} \vec{W}_n A^n, \quad (9)$$

where $A \triangleq \left(\begin{smallmatrix} 1 & T/N \\ 0 & 1 \end{smallmatrix}\right)$. Equation (9) can be solved by vectorizing $\overleftarrow{W}_{\tilde{X}_{k+1}}$. Similarly, the weighted mean $\overleftarrow{W}_{\tilde{X}_{k+1}} \overleftarrow{m}_{\tilde{X}_{k+1}}$ can be calculated as

$$\overleftarrow{W}_{\tilde{X}_{k+1}} \overleftarrow{m}_{\tilde{X}_{k+1}} = \left(I - \beta\rho^T \left(A^N\right)^{\mathrm{T}}\right)^{-1} \sum_{n=1}^{N} \rho^{nT/N} (A^n)^{\mathrm{T}} \vec{W}_n \vec{m}_n. \quad (10)$$

Parameter		Offline	Online
N	No. connect. in period. mod.	9	9
θ	Threshold	10	23
ρ	Forget. fact. smooth model	10^{-8}	10^{-8}
β	Forget. fact. period. model	0.9	0.9
σ_0^2	"Rainy" noise variance	12.25	12.25
σ_1^2	"Dry" noise variance	0.01	0.01
$\sigma_{U,0}^2$	Connection noise var.	0.16	0.16
$\sigma_{U,1}^2$	Connection noise var.	1	1
R_1, R_2	Recursions	5, 2	–

Table 1: Parameters of the model and the algorithms

(Note that $(\cdot)^{\mathrm{T}}$ means matrix transposition, while $(\cdot)^T$ raises a quantity to the power of the period T.)

The algorithm (with reference to Figures 2–5) is the following:

1. Initialize the algorithm by setting $\vec{\mu}_{X_0}(x) = 1$ and $\vec{\mu}_n(s) = 1$ for all $n = 1, \ldots, N$. Let $k = 0$.
2. Assign $k' := k$, i.e., all processing has been done until and including time $t_{k'}$. Fetch the next data item y_k with time stamp t_k.
3. For each $\ell \in \mathcal{L} \cap \{k'+1, k'+2, \ldots, k-1\}$ chose $\ell' \in \mathcal{L}$ such that $t_{\ell'} = t_\ell - T$ and do the following:
   (a) From $\vec{\mu}_{X_{\ell-1}}$ (assuming $\overleftarrow{\mu}_{X_\ell}$ is neutral) calculate $\overleftarrow{\mu}_{\tilde{S}_\ell}$. From $\vec{\mu}_{S_{\ell'}}$ and $\overleftarrow{\mu}_{\tilde{S}_\ell}$ calculate $\vec{\mu}_{S_\ell}$.
   (b) From $\vec{\mu}_{S_{\ell'}}$ (assuming $\overleftarrow{\mu}_{S_\ell}$ is neutral) calculate $\vec{\mu}_{\tilde{S}_\ell}$. From $\vec{\mu}_{\tilde{S}_\ell}$ and $\vec{\mu}_{X_{\ell-1}}$ calculate $\vec{\mu}_{X_\ell}$. Let $[\hat{x}_\ell]_1 = \left[\vec{m}_{X_\ell}\right]_1$.
4. Calculate $\overleftarrow{\mu}_{\tilde{X}_{k+1}}$ according to in (9) and (10). From $\overleftarrow{\mu}_{\tilde{X}_{k+1}}$ calculate $\overleftarrow{\mu}_{X_k}$ (Figure 4). From $\overleftarrow{\mu}_{X_k}$ and $\vec{\mu}_{X_{k-1}}$ calculate $\vec{\mu}_{\tilde{Y}_k}$ (Figure 3). Calculate the estimate $\hat{y}_k$ and the class label c_k according to (7) and (8) respectively.
5. Go to Step 2.

4. RESULTS

Both algorithms have been applied to real-world data, of which we report the following example. In this example, the microwave link operates at a single frequency of 38 GHz and covers a distance of 2876 m. The link gain is provided in units dBm in irregular time intervals of approximately 3 min with a quantization of 0.1 dBm. Part of the data was deleted on purpose to examine the behavior of the algorithms in the

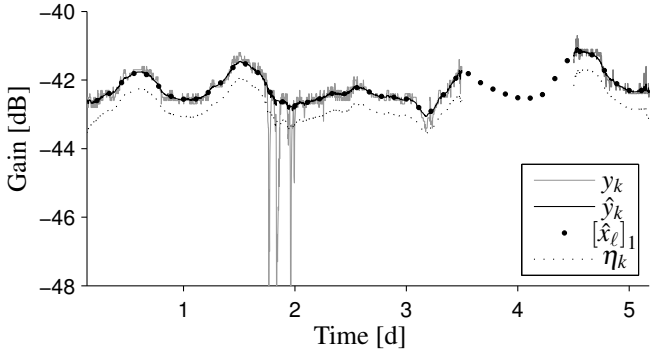

Figure 6: Offline algorithm

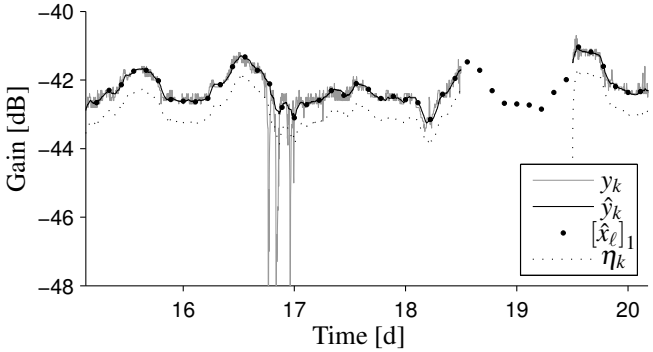

Figure 7: Online algorithm

case of missing data. The algorithm parameters were set as in Table 1.

Figures 6 and 7 show y_k (gray) and $\hat{y}_k$ (solid) at time instants t_k for $k \in \mathcal{K}$, and $[\hat{x}_\ell]_1$ (points) at time instants t_ℓ for $\ell \in \mathcal{L}$ both for the offline and the online algorithm respectively. For illustration the classification threshold η_k at time instants t_k for $k \in \mathcal{K}$ is shown as dotted lines. Both figures depict the same time window and the same measured data. While the online algorithm uses this data window exclusively, the offline algorithm was started 15 days earlier in order to train the "periodic" sub-model.

Figure 8 shows rain estimates obtained with the offline algorithm. (When compared with Figure 6, the time axes is zoomed onto the rain event.) These estimates are not optimized in any way: We simply take as an estimate of the rain rate the offset $y_k - \hat{y}_k$ for time instants t_k, $k \in \mathcal{K}$, at which we classify $c_k = 0$. The measured rainfall in Figure 8 is taken from a rain gauge nearby, which, however, is not a perfect ground truth [3].

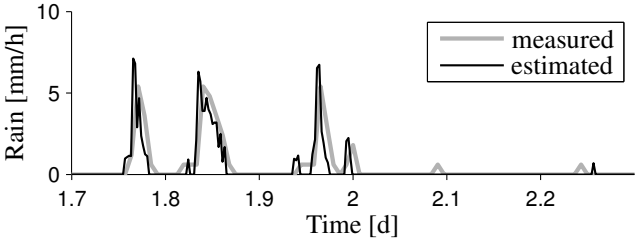

Figure 8: Estimated rain for offline algorithm

5. CONCLUSION AND OUTLOOK

We have described a factor graph representation of a stochastic model for quasi-periodic signals and we have devised algorithms based on the factor graph. Surprisingly, convergence seems to be fast despite the many loops.

To our best knowledge, this seems to be the first model which takes the daily cycle in microwave link attenuation data into account. For the example data, both algorithms were found to work satisfactorily. However, the offline version learns a more consistent "periodic" sub-model than the online version.

In further developments of this model, it might be valuable to include maximum likelihood estimates of the noise variances σ_0^2, σ_1^2, $\sigma_{U,0}^2$, and $\sigma_{U,1}^2$. For rainfall estimation, the inclusion of an existing dynamical model of rain attenuation (e.g. [7]) might be considered. Finally, the combination of attenuation data from multiple microwave links could make the algorithm more robust.

REFERENCES

[1] R. Olsen, D. Rogers, and D. Hodge, "The aR^b relation in the calculation of rain attenuation," *IEEE Trans. Antennas Propag.*, vol. 26, no. 2, pp. 318–329, 1978.

[2] G. Upton, A. Holt, R. Cummings, A. Rahimi, and J. Goddard, "Microwave links: The future for urban rainfall measurement?" *Atmospheric Research*, vol. 77, no. 1–4, pp. 300–312, 2005.

[3] H. Leijnse, R. Uijlenhoet, and J. N. M. Stricker, "Hydrometeorological application of a microwave link: 2. precipitation," *Water Resour. Res.*, vol. 43, no. 4, pp. W04 417–, Apr. 2007.

[4] O. Goldshtein, H. Messer, and A. Zinevich, "Rain rate estimation using measurements from commercial telecommunications links," *IEEE Trans. Signal Process.*, vol. 57, no. 4, pp. 1616–1625, 2009.

[5] M. Schleiss and A. Berne, "Identification of dry and rainy periods using telecommunication microwave links," *IEEE Geosci. Remote Sens. Lett.*, vol. 7, no. 3, pp. 611–615, 2010.

[6] H. Leijnse, R. Uijlenhoet, and J. N. M. Stricker, "Rainfall measurement using radio links from cellular communication networks," *Water Resour. Res.*, vol. 43, no. 3, pp. W03 201–, Mar. 2007.

[7] T. Maseng and P. Bakken, "A stochastic dynamic model of rain attenuation," *IEEE Trans. Commun.*, vol. 29, no. 5, pp. 660–669, 1981.

[8] H.-A. Loeliger, L. Bolliger, C. Reller, and S. Korl, "Localizing, forgetting, and likelihood filtering in state-space models," in *Proc. Information Theory and Applications Workshop*, 2009, pp. 184–186.

[9] I. Trajkovic, C. Reller, M. Wolf, and H.-A. Loeliger, "Modelling and filtering almost periodic signals by time-varying Fourier series with application to near infrared spectroscopy," in *Proc. 17th European Signal Proc. Conf. (EUSIPCO)*, 2009, pp. 632–636.

[10] H.-A. Loeliger, J. Dauwels, J. Hu, S. Korl, L. Ping, and F. R. Kschischang, "The factor graph approach to model-based signal processing," *Proc. IEEE*, vol. 95, no. 6, pp. 1295–1322, 2007.